Journal of Statistical Physics, Vol. 113, Nos. 1/2, October 2003 (© 2003)

A Boltzmann Equation Approach to the Dynamics of the Simple Piston

Christian Gruber[1] **and Gary P. Morriss**[2]

Received July 22, 2002

The evolution of a simple piston under a constant external force is investigated from a microscopic approach. Using Boltzmann's equation and simplifying assumptions it is shown that the system evolves towards equilibrium according to the macroscopic laws of thermodynamics: entropy production is positive and Onsager's relations are verified near equilibrium. Numerical simulations are presented which show that the evolution takes place in two stages: first a deterministic approach to the equilibrium position and then a stochastic motion around the equilibrium position. It also shows that the damping is not correctly described with these simplifying assumptions and a quantitative explanation of this effect remains an open problem.

KEY WORDS: Simple piston; Boltzmann equation; approach to equilibrium; entropy production; Onsager relations.

1. INTRODUCTION

There is a renewed interest in the theoretical understanding of the applicability of the second law of thermodynamics to small systems in particular, but also the nature of the approach to equilibrium and the identification of the entropy function far from equilibrium.[1] The focus of these studies is purely microscopic and the systems of interest are most usually those in which all of the constituents can be treated exactly in a classical mechanical sense. The time evolution can then be followed, in principle, exactly in a computer simulation and hence direct observations of the detailed approach to equilibrium can be made. The values of many properties such

[1] Institut de Physique Théorique, École Polytechnique Fédérale de Lausanne, CH-1015 Lausanne, Switzerland.

[2] School of Physics, University of New South Wales, Sydney NSW 2052, Australia; e-mail: G.Morriss@unsw.edu.au

0022-4715/03/1000-0297/0 © 2003 Plenum Publishing Corporation

as energy and pressure can easily be determined microscopically and the flow of energy and the establishment of mechanical and thermal equilibrium can be tracked. A model system of gas in a cylinder enclosed by a piston has been a standard tool in thermodynamics and through the Carnot cycle leads to the identification of entropy as a state function, so it is not surprising to find a microscopic approach to piston problems an important component of the latest studies.[2]

The "adiabatic" piston is a model system in which two regions of gas at initially different temperatures and pressures are separated by a piston. If the piston has no internal degrees of freedom then it is usually assumed to be unable to conduct heat, and is treated adiabatically.[3] However, when the mass of the piston is finite, energy is able to move from one region of gas to the other through the stochastic motion of the piston. It has been shown by qualitative arguments and numerical simulations[4, 5] that for a finite cylinder the evolution takes place in two stages with very different time scales. In the first stage the evolution is adiabatic and proceeds rapidly to mechanical equilibrium, where the pressures of the two gases are equal but the temperatures are not. Then the second stage is on a time scale several orders of magnitude longer, and leads to thermal equilibrium. These results have been recently established under simplifying assumptions using a two-time-scale perturbative approach.[6] However the mechanism responsible for the adiabatic evolution in the first stage is far from understood.

It is clear that the evolution of a simple piston, where the gas contained in one isolated cylinder is submitted to a constant force, is adiabatic and should exhibit properties similar to the first stage, i.e., the adiabatic evolution of a piston separating two fluids. Moreover, the simple piston is a trivial problem in thermodynamics for which the final equilibrium is immediately obtained from the two laws of thermostatics. Therefore, we expect that it will also be a simpler problem from a microscopical point of view and that it will lead to a better understanding of the mechanism responsible for the adiabatic evolution. In particular, one can expect that typically there will be a damped oscillation toward the equilibrium position characterized by a frequency and damping constant. This is the problem we address in this paper.

This adiabatic simple piston has a long history as E. Rüchardt in 1929[7] published a note containing a method of experimentally measuring the ratio of the specific heats of a gas $\gamma = C_p/C_v$. His apparatus used a large gas container connected to a precision made glass tube of uniform cross section, with a close fitting steel ball. When the steel ball is displaced from its equilibrium position and released it executes a damped oscillatory motion and the frequency of that motion can be directly related to the bulk modulus and then γ. Usually the oscillations are assumed to be adiabatic;

however, due to the finite thermal conductivities of the gas and the walls, there are heat flows into and out of the gas during expansion and compression and the system may be intermediate between adiabatic and isothermal.[8]

In an early report[9] on the simple two-dimensional piston with finite mass and finite amount of gas using numerical simulations, we observed two different regimes of damping behaviour—strong and weak damping—determined by the magnitude of the damping coefficient. It was clear that this damping coefficient is different from the friction coefficient responsible for the constant velocity initially observed when the damping is strong.

In this work we present a qualitative analysis of the results observed in the previous numerical simulations. Assuming as usual in kinetic theory that the correlation function has the factorisation property, we obtained from Boltzmann's equation the equations for the time evolution of the moments of the velocity of the piston (Section 2). In Section 3 we consider the thermodynamic limit for the piston where the width of the piston, and the number of particles N tend to infinity with N/L and $2mL/(M+m)$ fixed. In this limit we obtain deterministic equations for the piston. This equation is investigated first in the case of an infinite cylinder (Section 3.1), then for the finite cylinder (Section 3.2). The case of a piston with finite mass in an infinite cylinder is analysed in Section 4 and then in Section 5 we consider a piston with finite mass in a finite cylinder. As soon as the mass of the piston is finite we have to take into account fluctuations and the temperature of the piston. In this Section 5, connection with non-equilibrium thermodynamics is presented. Numerical simulations are presented and analysed in Section 6. Finally conclusions are elaborated in Section 7. It should be stressed that to obtain explicit equations for the evolution of the piston, without studying the motion of the gas, we have to introduce some *ad hoc* assumptions (Assumption 2 in Section 3 and Assumption 3 in Section 5). Those assumptions have been previously introduced in the analysis of experimental results. Our numerical simulations show that the equations so obtained predict correctly the frequency of oscillations, the friction effect in the first part of the evolution, and the strong vs. weak damping phenomena. However, it does not give an accurate prediction of the damping rate. Therefore the theory necessary to describe these intriguing numerical observations remains an open problem.

2. MICROSCOPIC MODEL: EQUATIONS FOR THE MOMENTS OF THE PISTON VELOCITY

The microscopic system we consider consists of N identical particles of mass m, moving in a two-dimensional rectangle (cylinder) of fixed width L,

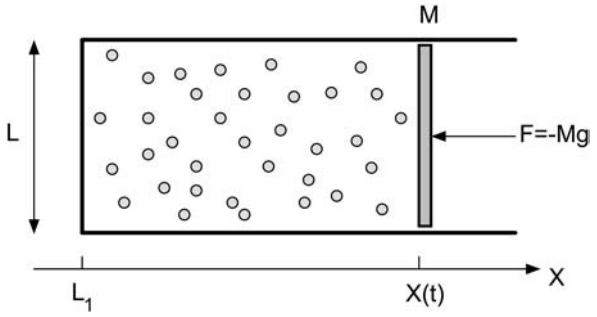

Fig. 1. The microscopic model; (L_1 will be either 0 or $-\infty$).

closed at one end by a fixed wall and on the other end by a movable piston of mass M. The walls and the piston are "adiabatic" in the sense that they have no internal degrees of freedom. (See Fig. 1.)

The piston moves without friction along the x-axis keeping its orientation fixed along the y-axis and it is submitted to a constant external force $F = -Mg$. In the following we shall consider a (partial) thermodynamic limit $L \to \infty$, $M \to \infty$, and $N \to \infty$ with

$$\gamma = \left(\frac{2mL}{M+m}\right) = \text{constant}, \qquad \frac{N}{L} = \text{constant}. \tag{1}$$

We denote $X(t)$ and $V(t)$ to be the position and velocity of the piston. They will be considered to be random variables. Let $\Phi(V; t)$ be the probability distribution for the velocity of the piston at time t; we shall be interested in the moments of the velocity:

$$\langle V^s \rangle_t = \int_{-\infty}^{\infty} dV\, \Phi(V; t)\, V^s. \tag{2}$$

The particles are hard-disks of diameter d making purely elastic collisions so that the kinetic energy is conserved during collisions, and

$$\frac{1}{M}\langle E_{\text{gas}} \rangle_t + \frac{1}{2}\langle V^2 \rangle_t + g\langle X \rangle_t = \text{constant}. \tag{3}$$

For example, with $\mathbf{v} \equiv (v, v_2)$ and V the velocities of a particle and the piston before a collision, then after the collision the velocities will be:

$$v' = -v + 2V + \frac{\gamma}{L}(v - V)$$

$$v_2' = v_2 \tag{4}$$

$$V' = V + \frac{\gamma}{L}(v - V).$$

The velocities of the particles are random variables and we introduce the density distribution of particles with velocity $\mathbf{v} \equiv (v, v_2)$ at the surface of the piston by

$$\rho(\mathbf{v}; t) = \rho(t)\, \varphi(\mathbf{v}; t) \tag{5}$$

with $\rho(t)$, twice the density of the particles which are going to hit the piston at time t, and

$$\int d\mathbf{v}\, \theta(v)\, \varphi(\mathbf{v}; t) = 1/2.$$

We assume the system to be homogeneous in the y-direction. We introduce the distribution of the velocity in the x-direction (by integrating out the y-component)

$$\varphi(v; t) = \int_{-\infty}^{\infty} dv_2\, \varphi(v, v_2; t) \qquad \int_0^{\infty} dv\, \varphi(v; t) = \tfrac{1}{2}.$$

For $t \leqslant 0$ the piston is rigidly fixed at some position X_0, i.e., $\Phi(V; t) = \delta(V)$, and the particles are in thermal equilibrium with density ρ_0 and temperature T_0 described by the Maxwellian distribution

$$\varphi(\mathbf{v}; t) = \left(\frac{m}{2\pi k_B T_0}\right) \exp\left(-\frac{m\mathbf{v}^2}{2k_B T_0}\right). \tag{6}$$

For $t \geqslant 0$ the piston moves freely under the action of the constant external force and the collisions with the particles. The problem is then to study the evolution of the piston.

In the following qualitative analysis we shall concentrate on the evolution of the piston and we shall introduce simplifying assumptions concerning the evolution of the gas. These assumptions generalize those which have been previously introduced to study experimental results[7, 8] and we expect that they will be satisfied for a dilute gas ($\rho(t)$ small with respect to the close-packing density) and small velocity of the piston

(compared to the velocities of the particles). In particular for this last condition to be satisfied the initial pressure exerted by the gas ($=\rho_0 k_B T_0$) should be approximately equal to the applied pressure ($=Mg/L$). We shall not try to justify these assumptions, but as we shall see the results obtained will be consistent with these assumptions and we shall compare the predicted consequences with the observed numerical simulations.

Assumption 1. Before the collision of a particle on the piston, it is possible to neglect the correlations between the velocity of the piston and the velocities of the particles: i.e., the two point correlation function $\rho(v, V; t)$ for the velocity of one particle which is going to hit the piston, and the velocity of the piston, has the factorisation property $\rho(v, V; t) = \rho(v; t)\, \Phi(V; t)$ if $v > V$.

Under this assumption we obtain from the Boltzmann equation (see ref. 10):

$$\frac{d}{dt}\langle V^s\rangle = -sg\langle V^{s-1}\rangle + L\left\langle \int_V^\infty dv\, \rho(t)\, \varphi(v; t)(v-V)\left\{\left[V+\frac{\gamma}{L}(v-V)\right]^s - V^s\right\}\right\rangle \tag{7}$$

where $\langle \cdots \rangle$ is the average computed with the distribution $\Phi(V; t)$. Let us define J_n which is a function of V and a functional of $\varphi(v; t)$ by

$$J_n(V) = J_n[V; \varphi] = \frac{(-1)^n}{n!}\int_V^\infty dv\, \varphi(v; t)(v-V)^n, \qquad n \geqslant 0. \tag{8}$$

Thus we have

$$\frac{d}{dt}\langle V^s\rangle = -sg\langle V^{s-1}\rangle + \gamma\rho(t)\sum_{n=0}^{s-1}(-1)^n\left(\frac{\gamma}{L}\right)^n \frac{s!\,(n+2)}{(s-n-1)!}\langle V^{s-n-1}J_n(V)\rangle. \tag{9}$$

This is the final equation we want to consider to study the evolution. In particular for $s = 1$, we have

$$\frac{d}{dt}\langle V\rangle = -g + 2\gamma\rho(t)\langle J_2(V)\rangle = -g + \frac{1}{M}F^{\text{gas}\to\text{piston}}. \tag{10}$$

Therefore we are led to define a "temperature," a "pressure," and a "friction coefficient" $\bar{\lambda}(V)$, at the surface of the piston by

$$k_B T = 4mJ_2(V=0) = 2m \int_0^\infty dv\, \varphi(v;t)\, v^2 \tag{11}$$

$$p = \rho k_B T \tag{12}$$

$$\bar{\lambda}(V)\, V = -2\gamma\rho(J_2(V) - J_2(0)). \tag{13}$$

It should be stressed that Eqs. (11)–(13) are simply definitions of quantities at the surface of the piston. In particular from Eq. (10) p is not the force per unit length exerted by the gas, and ρ is not the density of particles at the surface of the piston. In fact in the following we shall identify ρ with a function of the density of particles (see Eq. (17)). Therefore (12) should not be considered as the equation of state of a perfect gas. From (8) and (13), the friction coefficient is positive for all V (as it should be) and

$$\bar{\lambda}(V=0) = -2\gamma\rho J_1(V=0) = 2\gamma\rho \int_0^\infty dv\, \varphi(v;t)\, v. \tag{14}$$

In conclusion the force exerted by the gas on the piston is the sum of a pressure force, a friction force, and a force associated with the stochastic motion of the piston.

Property 1. The Maxwellian distribution functions

$$\begin{aligned} \varphi(v;t) &= \left(\frac{m}{2\pi k_B T}\right)^{\frac{1}{2}} \exp\left[-\frac{mv^2}{2k_B T}\right] \\ \Phi(V;t) &= \left(\frac{M}{2\pi k_B T}\right)^{\frac{1}{2}} \exp\left[-\frac{MV^2}{2k_B T}\right] \end{aligned} \tag{15}$$

define an equilibrium state of (7) if and only if

$$\frac{M}{L} g = \rho k_B T \tag{16}$$

where ρ is defined by Eq. (5) and is in general different from the density of particles.

This property is a direct consequence of Eq. (9), the explicit form of the Maxwellian distribution, and conservation of energy during collisions. It expresses the condition that the external force per unit length Mg/L balances the pressure exerted by the hard-disk gas $p = \rho k_B T$. From the simulations it follows that ρ can not be taken as the bulk density of

particles, but an excellent fit with the experimental results is obtained if we use Enskog's empirical formula for hard disks

$$\rho = n\frac{1+y^2/8}{(1-y)^2}, \qquad y = \frac{\pi d^2}{4}n \tag{17}$$

where n is the bulk density of particles.

In the following sections we want to investigate the evolution of the piston with initial conditions given by a Maxwellian distribution for the particles, but $\Phi_0(V) = \delta(V - V_0)$ for the piston. In particular, we would like to understand for this microscopic model if there is an approach to equilibrium, if this final state coincides with the one predicted by thermodynamics, and if the results predicted by the model coincide with those observed experimentally.[8]

3. THERMODYNAMIC LIMIT FOR THE PISTON

In this section we consider the thermodynamic limit for the piston, i.e., $L \to \infty$, $M \to \infty$, $N \to \infty$, with $\gamma = 2mL/(M+m) = \text{constant}$ and $N/L = \text{constant}$. In this limit (9) becomes

$$\frac{d}{dt}\langle V^s\rangle = -sg\langle V^{s-1}\rangle + 2s\gamma\rho(t)\langle V^{s-1}J_2(v)\rangle \tag{18}$$

and the following property is easily established (similar to ref. 7).

Property 2. Let $V(t) = \mathfrak{I}_t(V)$ be the solution of

$$\begin{cases} \dfrac{d}{dt}V(t) = -g + 2\gamma\rho(t)\,J_2(V) \\ V(t=0) = V_0 \end{cases} \tag{19}$$

(with $\rho(t)$ and $J_2(V, t)$ given functions of t), then the solution of (18) with the initial condition $\Phi_0(V) = \delta(V - V_0)$, is

$$\langle V^s\rangle_t = V(t)^s. \tag{20}$$

In conclusion if $\Phi_0(V) = \delta(V - V_0)$ then in the thermodynamic limit there are no fluctuations and $V(t)$ is a deterministic function.

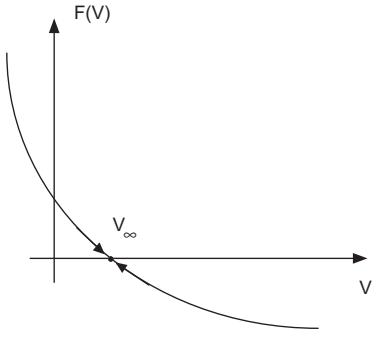

Fig. 2. The function $F(V)$.

3.1. Infinite Cylinder

Let us first consider the case of an infinite cylinder where $|L_1|$, as well as L, are infinite. We take initial conditions $\Phi_0(V) = \delta(V - V_0)$ and $\rho_0(v) = \rho_0 \varphi_0(v)$, with V_0, ρ_0, and $|1 - \frac{L}{Mg}\rho_0 k_B T_0|$ sufficiently small to neglect recollisions of the particles on the piston. In such a situation we expect that Assumption 1 will be satisfied and we can consider that the velocity distribution of particles before the collision on the piston will not vary in time so that $\rho(t) = \rho_0$ and $J_2(V; \varphi) = J_2(V; \varphi_0)$. In this case Eq. (19) has the form

$$\frac{dV}{dt} = F(V) \tag{21}$$

where

$$F(V) = -g + 2\gamma\rho_0 J_2(V; \varphi_0) = -g + \frac{L}{M}\rho_0 k_B T_0 - \bar{\lambda}(V)\, V.$$

Since

$$\frac{dF}{dV} = 2\gamma\rho_0 J_1(V) \leqslant 0$$

we have the following property.

Property 3. For the infinite system ($|L_1| = \infty$, $L = \infty$) the velocity of the piston $V(t)$ tends monotonically and exponentially fast to the value V_∞, the solution of

$$V_\infty \bar{\lambda}(V_\infty) = \frac{L}{M}\rho_0 k_B T_0 - g \tag{22}$$

and

$$\Phi_t(V) \to \delta(V - V_\infty).$$

Let us remark that Eq. (22), i.e.,

$$g = \frac{L}{M} 2m\rho_0 \int_{V_\infty}^{\infty} dv\, \varphi(v)(v - V_\infty)^2$$

expresses the condition that V_∞ is the velocity such that in the reference frame of the piston the pressure exerted by the gas is equal to Mg/L.

In particular, for a Maxwellian distribution of velocities the infinite system evolves towards a stationary state where the constant velocity V_∞ of the piston is given by the following implicit equation,

$$\begin{cases} g = \dfrac{L}{M} \rho_0 k_B T_0 \dfrac{4}{\sqrt{\pi}} \displaystyle\int_{\bar{u}}^{\infty} du\, e^{-u^2} (u - \bar{u})^2 \\ V_\infty = \sqrt{\dfrac{2k_B T_0}{m}}\, \bar{u}. \end{cases} \tag{23}$$

Clearly, if $|1 - \frac{L}{Mg} \rho_0 k_B T_0|$ is small, then V_∞ is small, approximately given by

$$V_\infty \cong \frac{1}{\rho_0} \sqrt{\frac{\pi}{8mk_B T_0}} \left[\rho_0 k_B T_0 - \frac{Mg}{L} \right]. \tag{24}$$

If moreover V_0 is small we can linearize (19) to obtain

$$V(t) \cong V_\infty + (V_0 - V_\infty)\, e^{-\bar{\lambda} t} \tag{25}$$

$$\bar{\lambda} = \frac{2L}{M} \rho_0 \sqrt{\frac{2mk_B T_0}{\pi}} = \bar{\lambda}(V = 0). \tag{26}$$

It is interesting to observe that the same problem in fluid dynamics (using a 1-dimensional shock wave[11]) gives

$$V_\infty = \frac{1}{\rho_0} \sqrt{\frac{1}{2mk_B T_0}} \left[\rho_0 k_B T_0 - \frac{Mg}{L} \right]$$

i.e., Eq. (24) with $\sqrt{\pi/8} \cong 0.627$ replaced by $1/\sqrt{2} = 0.707$. However, although describing the same physical situation, these equations have been derived using completely different set up. In fluid dynamics it is a consequence of the macroscopic continuity equations together with the adiabatic

condition, while in our approach it follows from a microscopic dynamics together with the condition that recollisions can be neglected and Assumption 1.

Let us note that for any stationary distribution of velocity for the particles, the infinite system evolves toward the stationary state $V(t) = V_\infty$. Furthermore the time necessary to reach this stationarity is of the order λ^{-1} and will be very short for large λ. From (22) this final state is an equilibrium state with $V_\infty = 0$, if and only if $\rho_0 k_B T_0 = Mg/L$ where T_0 is defined by (12).

3.2. Finite Cylinder

We consider again a piston with infinite mass $L = \infty$, but now the cylinder has finite length so that $\rho(t)$, $T(t)$, and $J_q(t)$ are functions of time. We put $L_1 = 0$. We take initial conditions such that for the piston $\Phi_0(V) = \delta(V - V_0)$ with $|V_0|$ small, and for the particles ρ_0 and $|1 - \frac{L}{Mg}\rho_0 k_B T_0|$ sufficiently small to expect that our assumptions will be valid.

In the analysis of the experimental results[7, 8] it was assumed that the thermodynamic quantities of the gas at the surface of the piston are approximately given by the average of those quantities in the gas, i.e., $\rho = N/L\langle X\rangle$ and $k_B T = \langle E_{\text{gas}}\rangle/N$. As we have discussed in Section 2, and is confirmed by the numerical simulations corresponding to Section 3.1 (infinite cylinder), one can not take ρ equal to $n = N/LX$ as soon as $n \geqslant 0.05$ (unit of length is hard core diameter). An excellent fit is however obtained if one considers ρ to be this function of n such that $p = \rho(n)\, k_B T$ is the equation of state of the gas. These remarks leads us to introduce the following assumption, whose validity will have to be tested by the simulations.

Assumption 2 (2-dimensional cylinder).

(a) The density of particles on the surface of the piston is given by

$$\rho(t) = \rho(X(t)), \tag{27}$$

where the function $\rho(X)$ has the following properties

$$\rho(X) > 0 \quad \text{and} \quad \frac{d\rho}{dX} < 0 \qquad \text{for} \quad X > X_{\min} \geqslant 0$$

$$\rho(X) = \infty \qquad \text{for} \quad X \leqslant X_{\min} \quad \text{(hard core packing)}.$$

For example, one can take[12]

$$\rho(X)=\frac{N}{LX} \qquad \text{or} \qquad \rho(X)=\frac{N}{L(X-a)} \qquad \text{or}$$

$$\rho(X)=\frac{N}{LX}\frac{1}{(1-c/X)^2} \qquad \text{or} \qquad \rho(X)=\frac{N}{LX}\frac{1+\frac{1}{8}(c/X)^2}{(1-c/X)^2}$$

with $c=\frac{\pi}{4}d^2N/L$, $a=2c$, (d is the diameter of the hard disk) which corresponds respectively to a very dilute gas, a dilute van der Waals gas, or a moderately dense Enskog gas of hard disks.

(b) The temperature T of the gas near the surface of the piston, defined by (12), is given by

$$\langle E_{\text{gas}}\rangle = Nk_BT. \tag{28}$$

With the initial condition $\Phi_0(V)=\delta(V-V_0)$, we have seen that $\langle V^s\rangle=\langle V\rangle^s$, and from (3), (19), and (28) we have

$$k_BT(t)+\frac{1}{2}\frac{M}{N}V(t)^2+\frac{M}{N}gX(t)=\frac{E_0}{N}=\text{constant} \tag{29}$$

$$\frac{d}{dt}V=-g+\frac{L}{M}\rho k_BT-\bar{\lambda}(V;t)\,V \tag{30}$$

with $\bar{\lambda}(V;t)\geqslant 0$. We thus have to discuss the evolution of $X(t)$ satisfying (29) and (30).

Property 4. The equilibrium states of the piston with infinite mass in a finite cylinder are uniquely given by

$$\begin{cases} \dfrac{M}{L}g=\rho(X_{\text{eq}})\,k_BT_{\text{eq}} \\ k_BT_{\text{eq}}=\dfrac{E_0}{N}-\dfrac{M}{N}gX_{\text{eq}} \end{cases} \tag{31}$$

that is

$$X_{\text{eq}}+\frac{N}{L}\frac{1}{\rho(X_{\text{eq}})}=\frac{E_0}{Mg}. \tag{32}$$

Property 5. Under Assumptions 1 and 2, the piston evolves toward the equilibrium state defined by (31).

Proof. From (29) and (30)

$$\frac{d}{dt}(k_B T) = -\frac{L}{N}\rho(X)\, k_B T \frac{dX}{dt} + \frac{M}{N}\bar{\lambda} V^2. \tag{33}$$

Let us introduce the function $F(X)$ by

$$\frac{d}{dX}\ln F(X) = \frac{L}{N}\rho(X). \tag{34}$$

Then from (33) we have

$$F(X_t)\, T_t = F(X_0)\, T_0 \exp\left[\int_0^t dt' \frac{M}{N}\frac{\bar{\lambda} V^2}{k_B T}\right] \tag{35}$$

which shows that the solution of (29) and (30) will satisfy the condition

$$T_t > 0 \quad \forall t \tag{36}$$

(as it should from the definition). The proof is then concluded with the help of the following lemma, which can easily be established.

Lemma 1. The function $S = S(E, X, V)$ defined by

$$S(E, X, V) = k_B \frac{N}{L}\ln\left[F(X)\left(\frac{E}{M} - gX - \frac{1}{2}V^2\right)\right] \tag{37}$$

i.e.,

$$S(T, X, V) = k_B \frac{N}{L}\ln\left[F(X)\, k_B T \frac{N}{M}\right] = S(T, X) \tag{38}$$

has the following properties under the evolution defined by (29) and (30).

1.

$$\frac{dS}{dt} = \frac{1}{T}\frac{M}{L}\bar{\lambda}(V)\, V^2 \geqslant 0. \tag{39}$$

2. The equilibrium point $(X_f, V_f = 0)$ defined by (31) is the unique maximum of the function $S(E, X, V)$ under the constraint $E = E_0$.

Conclusion. In the thermodynamic limit for the piston, i.e., $L \to \infty$, the evolution of the piston is deterministic. It is the adiabatic evolution of an adiabatic piston which satisfies the two laws of thermodynamics with $S(E, X, V)$ the entropy (per unit length) of the system. In fact from Eqs. (3), (10), and (20) we have the first law of thermodynamics

$$\frac{d}{dt}\langle E^{\text{gas}}\rangle = F^{\text{gas}\to\text{piston}} V$$

(independent of Assumption 2) which implies that the heat flux is zero, and the evolution defined by Eqs. (30) and (39), was derived in ref. 10 from the two laws of thermodynamics.

To compare the numerical simulations with the result obtained above we shall linearize Eqs. (30) and (39) around the equilibrium point $(X_f, V_f = 0)$. Introducing $\xi = X - X_f$ and using (31)

$$\frac{d^2}{dt^2}\xi = -g\left[\frac{L}{N}\rho_f - \left(\frac{\rho'}{\rho}\right)_f\right]\xi - \bar{\lambda}_f \frac{d}{dt}\xi \tag{40}$$

which yields

$$\xi(t) = e^{-\Omega t} \tag{41}$$

with

$$\Omega_{\pm} = \frac{1}{2}\left\{\bar{\lambda}_f \pm i\sqrt{4g\left[\frac{L}{N}\rho_f - \left(\frac{\rho'}{\rho}\right)_f\right] - (\bar{\lambda}_f)^2}\right\} \tag{42}$$

where $X_f + \frac{N}{L}\frac{1}{\rho(X_f)} = \frac{E_0}{Mg}$ and from (25) and (31)

$$\bar{\lambda}_f = \frac{2L}{M}\rho_f\sqrt{\frac{2m}{\pi}k_B T_f} = 2\sqrt{\frac{2m}{\pi}\frac{L}{M}\rho_f g}.$$

Taking the expression $\rho(X) = (N/LX)(1/(1-c/X)^2)$ from Assumption 2, in this case we have

$$\begin{aligned}
\omega_f^2 &= g\left[\frac{L}{N}\rho_f - \left(\frac{\rho'}{\rho}\right)_f\right] = \frac{g}{X_f}\frac{2-(c/X_f)^2}{(1-c/X_f)^2} = 2\frac{L^2}{MN}\rho_f^2 k_B T_f\left[1 - \frac{1}{2}\left(\frac{c}{X_f}\right)^2\right] \\
\bar{\lambda}_f &= \frac{2}{(1-c/X_f)}\sqrt{\frac{2m}{\pi}\frac{N}{M}\frac{g}{X_f}} = \frac{L}{M}\rho_f\sqrt{\frac{8mk_B T_f}{\pi}} \\
X_f &= \frac{c}{2}\left(1 + \frac{E_0}{2cMg}\right)\left[1 + \sqrt{1 - 2\left(1 + \frac{E_0}{2cMg}\right)^{-2}}\right]
\end{aligned} \tag{43}$$

where $E_0 = Nk_BT_0 + MgX_0$ and $k_BT_f = (E_0 - MgX_f)/N$ which implies

$$\omega_f^2 - \frac{1}{4}\bar{\lambda}_f^2 = \frac{g}{X_f}\frac{1}{(1-c/X_f)^2}\left[2 - \frac{2m}{\pi}\frac{N}{M} - \left(\frac{c}{X_f}\right)^2\right]. \tag{44}$$

Let us note that from those linearized equations it follows that there is a change in behaviour when $M_{\text{gas}}/M = Nm/M = \pi$: i.e., if $M_{\text{gas}}/M < \pi$ the damping is weak; if $M_{\text{gas}}/M > \pi$ the damping is strong.

4. PISTON WITH FINITE MASS IN AN INFINITE CYLINDER

In the next two sections, we consider the case where L, and thus M, is large but finite. We will assume the distribution $\Phi(V; t)$ has an asymptotic expansion in powers of (γ/L) which is uniform with respect to time and thus

$$\langle V^s \rangle_t = \sum_{n=0}^{\infty} \left(\frac{\gamma}{L}\right)^n v_{s,n}(t).$$

In Section 3 we have studied the solution at order zero. In the following we shall consider the evolution up to order one in the small parameter (γ/L). In this section we discuss first the case of the infinite cylinder, so that ρ, T, and $J_n[V; \varphi]$ do not depend on time.

Property 6. Let $V(t)$, $\Delta(t)$, be the solutions of

$$\begin{cases} \dfrac{d}{dt}V(t) = -g + 2\gamma\rho J_2(V) + \gamma\rho J_0(V)\,\Delta & (45) \\ \dfrac{d}{dt}\Delta(t) = 2\gamma\rho\left[2J_1(V)\,\Delta - 3\left(\dfrac{\gamma}{L}\right)J_3(V)\right] & (46) \end{cases}$$

with $V(0) = 0$ and $\Delta(0) = 0$, then the solution of (9) with initial conditions $\langle V^s \rangle_{t=0} = 0$ is given at order (γ/L) by

$$\langle V^s \rangle = V^s + \frac{s(s-1)}{2}V^{s-2}\Delta \tag{47}$$

where $\Delta(t) = \langle V^2 \rangle - \langle V \rangle^2 = O(\frac{\gamma}{L})$.

Corollary. The stationary solution of the piston with finite mass, in the infinite cylinder, is given at order (γ/L) by

$$g = \gamma\rho\left[2J_2(V_{st}) + \frac{3}{2}\left(\frac{\gamma}{L}\right)\frac{J_0(V_{st})\,J_3(V_{st})}{J_1(V_{st})}\right] \tag{48}$$

$$\Delta_{st} = \frac{3}{2}\left(\frac{\gamma}{L}\right)\frac{J_3(V_{st})}{J_1(V_{st})}. \tag{49}$$

As we have discussed in Section 3 (for $\gamma/L = 0$), if $|1 - L\rho_0 k_B T_0/Mg|$ is small, then V_∞ is small. Adding the term in γ/L in (9) we expect that for $\gamma/L \ll 1$ we have similarly $|V_{st}| \ll 1$ so that we can consider Eq. (48) to first order in V_{st}. Introducing $j_n = J_n(V = 0)$ and using the fact that $(d/dV)\,J_n(V) = J_{n-1}(V)$ we have

$$J_n(V) = \sum_{r=0}^{\infty} \frac{V^r}{r!}\, j_{n-r}.$$

Therefore to first order in V_{st} we obtain

$$g = \gamma\rho\left[2j_2 + 2j_1 V_{st} + \frac{3}{2}\left(\frac{\gamma}{L}\right)\frac{j_0 j_3}{j_1}\right] \tag{50}$$

$$\Delta_{st} = \frac{3}{2}\left(\frac{\gamma}{L}\right)\frac{j_3}{j_1}. \tag{51}$$

In particular taking as initial conditions Maxwellian distributions of velocities for the particles yields

$$j_0 \triangleq \frac{1}{2} \qquad j_1 \triangleq -\left(\frac{k_B T}{2\pi m}\right)^{1/2} \qquad j_3 \triangleq \frac{1}{3}\left(\frac{k_B T}{m}\right) j_1 \tag{52}$$

$$\Delta_{st} = \langle V^2\rangle_{st} - \langle V\rangle_{st}^2 = \frac{k_B T_0}{M} \tag{53}$$

$$\bar{\lambda} V_{st} = -g + \rho_0 k_B T_0 \frac{L}{M} \tag{54}$$

$$\bar{\lambda} = 2\gamma\rho_0 \sqrt{\frac{k_B T_0}{2\pi m}}. \tag{55}$$

To conclude this section, let us consider the evolution for the case where $|1 - (L/Mg)\,\rho k_B T| \ll 1$. Under this condition $|V_{st}| \ll 1$ and we can linearize (45) and (46) to obtain

$$\begin{cases} \dfrac{d}{dt} V(t) = -g + 2\gamma\rho j_2 + 2\gamma\rho j_1 V + \gamma\rho j_0(V)\, \Delta & (56) \\ \dfrac{d}{dt} \Delta(t) = 2\gamma\rho \left[2j_1 \Delta - 3\left(\dfrac{\gamma}{L}\right) j_3 \right] & (57) \end{cases}$$

where by definition $2\gamma\rho j_2 = \frac{\gamma}{2m}\rho k_B T = \frac{L}{M+m}\rho k_B T$.

Property 7. Under the condition $|1-(L/Mg)\,\rho k_B T| \ll 1$ and the initial condition $\Phi_0(V) = \delta(V)$ the evolution of the piston with finite but large mass in the infinite cylinder is given at first order in (γ/L) by

$$\begin{aligned} \langle V^2 \rangle_t - \langle V \rangle_t^2 &= \frac{\gamma}{L} \frac{3j_3}{2j_1} (1 - e^{-2\bar{\lambda}t}) \\ \langle V \rangle_t &= \frac{1}{\bar{\lambda}} \left(\frac{\gamma}{2m} \rho k_B T - g \right) (1 - e^{-\bar{\lambda}t}) - \frac{\gamma}{L} \frac{3 j_0 j_3}{4 j_1^2} (1 - e^{-\bar{\lambda}t})^2 \end{aligned} \tag{58}$$

where $\bar{\lambda} = 2\gamma\rho\,|j_1|$.

Conclusion.

1. Under the condition $|1-(L/(M+m)\,g)\,\rho_0 k_B T_0| \ll 1$, the piston will reach equilibrium, i.e., $\langle V \rangle_{t\to\infty} = 0$ if and only if

$$g = \frac{L}{M+m} \rho k_B T + \frac{3}{2} \left(\frac{2m}{M+m} \right)^2 L\rho \frac{j_0 j_3}{j_1}. \tag{59}$$

In particular for a Maxwellian distribution the condition to reach equilibrium is from (52)

$$g = \frac{L}{M} \rho k_B T. \tag{60}$$

However for a stationary distribution of the molecules $\varphi(v) = f(v^2)$, which is not Maxwellian the condition for equilibrium is (59) and not (60).

2. Defining the temperature of the piston by

$$k_B T_{\text{piston}} = M[\langle V^2 \rangle - \langle V \rangle^2] \tag{61}$$

it follows from (53) that in the stationary state $T_{\text{piston}} = T$.

3. If $|1-(L/Mg)\,\rho_0 k_B T_0| = O(\gamma)$ then $\langle V \rangle = O(\gamma)$, but $\langle V^2 \rangle - \langle V \rangle^2 = O(\gamma/L)$. In this case the motion is deterministic and the fluctuations are

negligible. On the other hand if $|1-(L/Mg)\,\rho_0 k_B T_0| = O(\gamma/L)$ then $\langle V\rangle = O(\gamma/L)$ and $\langle V^2\rangle - \langle V\rangle^2 = O(\gamma/L)$ and in this case the fluctuations are important.

5. PISTON WITH FINITE MASS IN A FINITE CYLINDER

From Boltzmann's Equation to Thermodynamics

As in Section 3.2 we take $L_1 = 0$. Let us recall that by definition Eq. (13)

$$4m\rho J_2(V) = p - \frac{M+m}{L}\,\bar{\lambda}(V)\,V. \tag{62}$$

We now introduce a second friction coefficient $\zeta(V)$ defined by

$$2\rho J_0(V) = \rho - \frac{M}{L}\frac{\zeta(V)}{k_B T}\,V \tag{63}$$

which is positive for all V, since $j_0 = \frac{1}{2}$ and $dJ_0(V)/dV = -\varphi(V;t)$ is negative.

The evolution at order γ/L is such that Eq. (45) and (46) are satisfied with $V = dX/dt = \langle V\rangle$ and $\Delta(t) = \langle V^2\rangle - \langle V\rangle^2 = k_B T_{\text{piston}}/M$. Therefore the *equilibrium states* are characterized by

$$\begin{cases} \langle V\rangle = 0 \\ \langle V^2\rangle = \Delta = \dfrac{3}{2}\dfrac{\gamma}{L}\dfrac{j_3}{j_1} = \dfrac{3m}{M+m}\dfrac{j_3}{j_1} \\ g = \gamma\rho\left(\dfrac{k_B T}{2m} + \dfrac{3}{2}\dfrac{m}{M+m}\dfrac{j_3}{j_1}\right) \end{cases} \tag{64}$$

(which is the same as (48) and (49) with $V_{\text{st}} = 0$).

At this point we can not say anything about j_1 and j_3. However, for initial conditions such that the distribution of velocities are Maxwellian with $L\rho_0 k_B T_0 \approx Mg$ and $\phi(V) = \delta(V)$, the initial state differs from an equilibrium state only because Δ^2 is zero, instead of being equal to $k_B T_0/M = O(\gamma/L)$. Taking for initial conditions Maxwellian distributions with $|1 - L\rho_0 k_B T_0/Mg| \ll 1$ and $\phi(V) = \delta(V - V_0)$ with $|V_0| \ll 1$, we expect that the velocity of the piston will remain small and that the relation between J_1 and J_3 will remain the same as for Maxwellian velocities at order zero in γ/L. Thus we introduce

Assumption 3. For $|V| \ll 1$, the relation between J_1, J_2, and J_3 is at order zero in γ/L, the same as for Maxwellian distributions, i.e.,

$$-6mJ_3(V)+2mVJ_2(V)=-2k_BTJ_1(V)+O\left(\frac{\gamma}{L}\right) \tag{65}$$

which implies for $V=0$

$$3mj_3=k_BTj_1+O\left(\frac{\gamma}{L}\right) \qquad \text{with} \quad j_1=-\sqrt{\frac{k_BT}{2\pi m}}. \tag{66}$$

With this last assumption, the equilibrium states are characterized by

$$\begin{cases} \langle V\rangle = 0 \\ \langle V^2\rangle = \dfrac{k_BT}{M} \\ g=\dfrac{L}{M}\rho k_BT \end{cases} \tag{67}$$

and therefore at equilibrium the temperature of the piston, defined by (61), is equal to the temperature of the gas.

To discuss the evolution we note that since L_1 is finite the functions $J_1(V)$, $J_2(V)$, $J_3(V)$ will depend on time. Therefore we should consider the Boltzmann equation for the fluid with time dependent boundary conditions to obtain $\varphi(v;t)$. Before investigating this difficult problem and to get some feeling about the equations describing the evolution, we consider that Assumptions 1–3 hold at order zero at least for some initial conditions close to the equilibrium condition. With those three assumptions the evolution (45) and (46) is described to first order in the small parameter $\alpha=\gamma/L=2m/(M+m)$ by the equations

$$\begin{cases} \dfrac{d}{dt}V=-g+\dfrac{L}{M}\rho k_BT-\bar{\lambda}(V)\,V-\dfrac{\alpha}{2}\left[\dfrac{L}{M}\rho k_B(T-T_p)+\dfrac{T_p}{T}\zeta(V)\,V\right] \\ \dfrac{d}{dt}(k_BT_p)=8m\dfrac{L}{M}\rho k_B(T_p-T)\,J_1(V)-2m\dfrac{L}{M}\rho k_BTV+2m\bar{\lambda}(V)\,V^2 \end{cases} \tag{68}$$

where $\rho=\rho(X)$ is given by (27) and T_p is the piston temperature, together with the equation for conservation of energy (and Assumption 2)

$$\frac{N}{M}k_B\frac{d}{dt}T+V\frac{d}{dt}V+\frac{1}{2}\frac{d}{dt}\Delta+gV=0. \tag{69}$$

Furthermore we introduce the temperature T and the entropy S for the gas and the piston by:

For the gas (as in Section 3.2 except that here it is not per unit length)

$$\begin{aligned} E_g &= Nk_BT, \\ S_g &= Nk_B \ln[F(X)\, Nk_BT] \end{aligned} \tag{70}$$

where $\frac{d}{dX} \ln F(X) = \frac{L}{N} \rho(X)$.

For the piston (from (61))

$$E_p = \tfrac{1}{2} M\langle V^2\rangle = \tfrac{1}{2} MV^2 + \tfrac{1}{2} k_BT_p \tag{71}$$

$$S_p = \tfrac{1}{2} k_B \ln(k_BT_p). \tag{72}$$

For the whole system

$$E = E_g + E_p + MgX \tag{73}$$

$$\begin{aligned} S &= S_g + S_p = Nk_B \ln[F(X)(E - MgX - E_p)] + \tfrac{1}{2} k_B \ln[2E_p - MV^2] \\ &= S(E, E_p, X, V). \end{aligned} \tag{74}$$

Property 8. The equilibrium state of the evolution Eq. (68), is given by Eq. (67) and correspond to the unique maximum of the entropy function $S(E, E_p, X, V)$ under the constraint that $E = E_0$ is fixed. The proof is straightforward and will be omitted.

To study the evolution we consider the "entropy production" dS/dt. From (74) we have

$$\frac{dS}{dt} = \left\{ k_BL\rho(X) - \frac{M}{T}\left(\frac{d}{dt}V + g\right)\right\} V - \left\{\frac{1}{T} - \frac{1}{T_p}\right\}\left(\frac{1}{2} k_B \frac{d}{dt} T_p\right). \tag{75}$$

On the other hand defining a "dissipative force" F_{diss} by Newton's equation

$$\frac{d}{dt}\langle V\rangle = -g + \frac{L}{M}(p + F_{\text{diss}}) \tag{76}$$

and a "heat flux" J_Q by the 1st law of thermodynamics

$$\frac{d}{dt}\left(\frac{\langle E^{\text{gas}}\rangle}{L}\right) = -(p + F_{\text{diss}})\langle V\rangle + J_Q^{p \to \text{gas}} \tag{77}$$

we obtain from Eqs. (76), (77), (71) and the conservation of energy (3)

$$J_Q^{p\to\text{gas}} = -\frac{k_B}{2L}\frac{d}{dt}T_p = -J_Q^{\text{gas}\to p}. \tag{78}$$

Moreover from Eqs. (45) and (46) (i.e., Boltzmann's equation to first order in $\alpha = \gamma/L$) together with the definitions (62), (63), (61) and Eq. (78), we have

$$J_Q^{p\to\text{gas}} = \alpha\rho\left[-2k_BT_pJ_1(V) + \frac{M}{M+m}\,6mJ_3(V)\right] \tag{79}$$

$$-F_{\text{diss}} = -\frac{\alpha}{2}\rho k_BTT_p\left[\frac{1}{T}-\frac{1}{T_p}\right] + \frac{M}{L}\left[T\bar{\lambda}(V) + \frac{\alpha}{2}T_p\zeta(V)\right]\frac{V}{T} \tag{80}$$

and from Eqs. (78) and (75) (derived using Assumption 2)

$$\frac{d}{dt}\left(\frac{S}{L}\right) = J_Q^{p\to\text{gas}}\left[\frac{1}{T}-\frac{1}{T_p}\right] - F_{\text{diss}}\frac{V}{T}. \tag{81}$$

This last equation is of the form

$$\frac{d}{dt}\left(\frac{S}{L}\right) = \sum_{\alpha=1}^{2} J_\alpha X_\alpha = (\mathbf{J},\mathbf{X}) \tag{82}$$

with

$$\mathbf{J} = \begin{pmatrix} J_Q^{p\to\text{gas}} \\ -F_{\text{diss}} \end{pmatrix} \qquad \text{and} \qquad \mathbf{X} = \begin{pmatrix} \dfrac{1}{T}-\dfrac{1}{T_p} \\ \dfrac{V}{T} \end{pmatrix}. \tag{83}$$

Finally with Assumption 3, Eq. (79) yields

$$J_Q^{p\to\text{gas}} = 2\alpha\rho k_BTT_p\,|J_1(V)|\left[\frac{1}{T}-\frac{1}{T_p}\right] + 2\alpha m\frac{M}{M+m}\rho TJ_2(V)\frac{V}{T}. \tag{84}$$

In conclusion the entropy production per unit length is

$$\frac{d}{dt}\left(\frac{S}{L}\right) = \sum_{\alpha=1}^{2} J_\alpha X_\alpha \tag{85}$$

where

$$J_\alpha = \sum_{\beta=1}^{2} L_{\alpha\beta} X_\beta \tag{86}$$

and the matrix of coefficients is given by

$$\mathbf{L} = \begin{pmatrix} 2\alpha\rho k_B T T_p \, |J_1(V)| & 2\alpha m \rho T J_2(V) \\ -\frac{\alpha}{2} \rho k_B T T_p & \frac{M}{L}\left[T\bar{\lambda}(V) + \frac{\alpha}{2} T_p \zeta(V) \right] \end{pmatrix}.$$

With (62) the form (85) will thus be positive definite if

$$32 \frac{M}{L} \rho k_B T_p \, |J_1(V)| \left[\bar{\lambda}(V) + \frac{\alpha}{2} \frac{T_p}{T} \zeta(V) \right]$$
$$\geqslant \alpha \left[\rho k_B (T - T_p) - \left(\frac{M+m}{L} \right) \bar{\lambda}(V) \, V \right]^2. \tag{87}$$

We remark that the left-hand side is strictly positive of order zero in α, while the right-hand side is of order one in α and zero for the equilibrium state $T = T_p$, $V = 0$.

Property 9. The evolution, defined by the Boltzmann equation to first order in α together with Assumptions 2 and 3, will satisfy the condition

$$\frac{dS}{dt} \geqslant 0 \qquad \text{for all } t$$

if the initial state is sufficiently near an equilibrium state (i.e., if the inequality (87) is satisfied for all t). In this case the piston will evolve to the unique equilibrium state associated with the maximum of S under the constraint of constant energy $E = E_0$.

Comments on the Thermodynamics

1. In the thermodynamic limit $L \to \infty$, $M \to \infty$, i.e., $\alpha = 0$ we recover the results of Section 3.2

$$J_Q^{p \to \text{gas}} = 0 \qquad \text{and} \qquad \frac{d}{dt}\left(\frac{S}{L}\right) = \frac{1}{T}\left(\frac{M}{L}\right) \bar{\lambda}(V) \, V^2.$$

The evolution of the gas is thus adiabatic (no heat transfer).

2. The evolution of the total system, as well as both sub-systems, obeys the two laws of thermodynamics.

3. From (72) and (78)

$$\frac{d}{dt} S_p = \frac{L}{T_p} J_Q^{\text{gas} \to p}$$

which shows that the variation of entropy of the piston is entirely due to the heat flux (no internal entropy production). On the other hand for the gas

$$\frac{d}{dt} S_g = \frac{L}{T} J_Q^{p \to \text{gas}} + \frac{1}{T} M \bar{\lambda}(V) V^2$$

and thus the variation of entropy of the gas is associated with the heat flux as well as an internal entropy production.

4. We observe a "coupling effect" between the two generalized forces (X_1, X_2) and the generalized fluxes (J_1, J_2), i.e., a non-zero velocity of the piston contributes to the heat flux, and a non-zero temperature difference contributes to the dissipative force.

5. The matrix **L** connecting the fluxes to the forces, evaluated at equilibrium, i.e.,

$$\mathbf{L} = \begin{pmatrix} 2\alpha\rho k_B T^2 |J_1(V)| & \frac{1}{2}\alpha\rho k_B T^2 \\ -\frac{1}{2}\alpha\rho k_B T^2 & \frac{M}{L} T \left[\bar{\lambda}(0) + \frac{\alpha}{2} \zeta(0) \right] \end{pmatrix}$$

is antisymmetric. We thus see that Onsager's relation is satisfied, with the anti symmetry property related to the fact that V changes sign under time reversal.

6. NUMERICAL RESULTS

The motion of the two-dimensional adiabatic piston containing a gas of hard particles (shown in Fig. 1), was simulated using the standard molecular dynamics method for hard disk systems. The length and mass scales in the simulation were determined by choosing the mass of each hard disk m and its diameter d to be equal to unity. We begin with an initial

arrangement of N non-overlapping hard disks with velocities chosen randomly, but so that the total kinetic energy of the gas is related to the desired initial temperature by

$$\frac{1}{2}\sum_{i=1}^{N} mv_i^2 = Nk_B T_0.$$

This system was evolved in time by determining the next collision event. Each particle moves in a straight line and the piston falls freely under the external force, until a collision occurs. This can be either a particle-particle collision, or a particle-wall collision, where the wall can be any of the cylinder walls or the piston. Once the next collision is reached, the collision rules (4) are used to find the post collision velocities of the particles, or particle and piston. Then the next collision is determined and the process is repeated for as many collisions as we desire.

In a typical numerical experiment, the cylinder contains N hard disks at some initial temperature kT_0, and the piston is at an initial position X_0. The piston is released, and generally the pressure exerted by the gas on the piston does not balance the force per unit length exerted by the piston on the gas. Thus the piston moves towards the final equilibrium position X_f. The system is evolved in time for a large number of collisions, and when the initial volume is such that the system is not in equilibrium we typically observe an evolution of the piston in two stages: first a damped oscillatory deterministic relaxation towards the equilibrium position, and then fluctuations around that equilibrium position (as in Fig. 3).

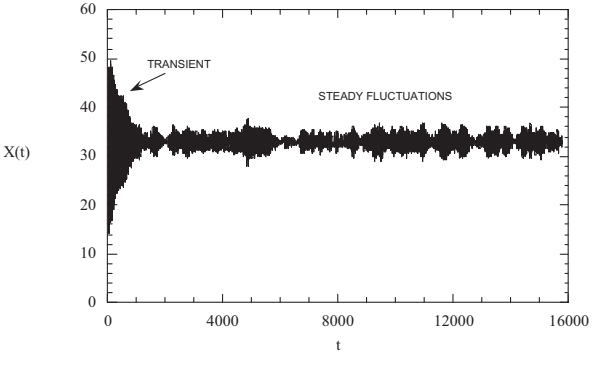

Fig. 3. The piston simulation of a hard disk gas of 108 particles with an initial temperature of 10 and initial density of 0.1. The piston mass is 500 and $g = 0.4$. The simulation shows two distinct behaviours: first an initial transient evolution where the piston performs a deterministic damped oscillation about the final equilibrium position X_f, then the piston fluctuates about the equilibrium position X_f.

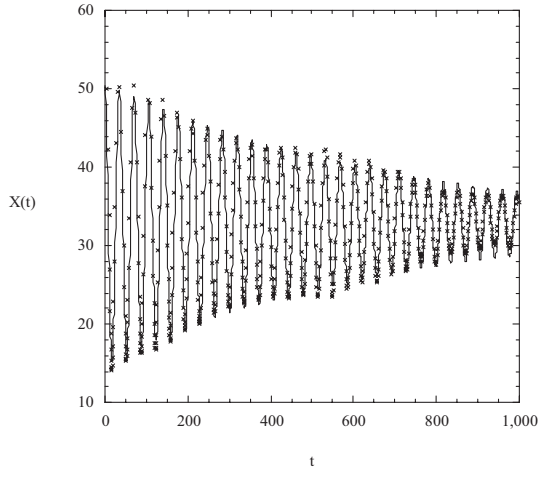

Fig. 4. The same data as in Fig. 3 with the time axis expanded to see the damped oscillatory behaviour more clearly. The simulation results are the crosses and the full line is the damped cosine fit.

Looking closer at the two regions we find that the transient motion (see Fig. 4) is, to a good approximation, a damped oscillation about the final equilibrium position with a well-defined frequency and damping constant $X(t) = X_f + (X_0 - X_f)\cos(\omega t)\exp(-\lambda t)$. Fitting the data to a damped cosine we can usually obtain a good estimate of both the frequency ω and the damping constant λ.

However, in the steady fluctuation region of Fig. 3, as enlarged in Fig. 5, we observe again a dominant single frequency of the motion of the

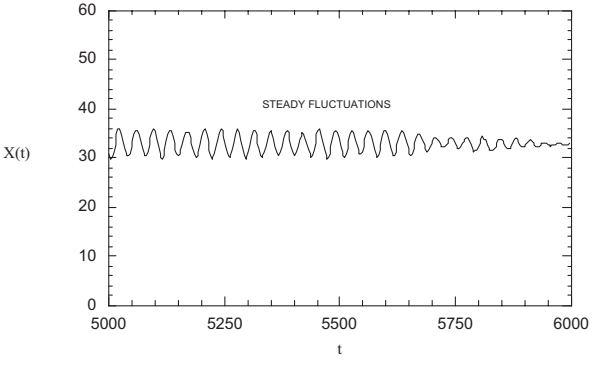

Fig. 5. The same data as in Fig. 3 with the time axis expanded to see the frequency of the piston fluctuations about the final equilibrium position.

piston, and that frequency is the same as the frequency of the motion in the transient region. The amplitude of the steady frequency oscillations in the fluctuation region is modulated seemingly at random, with occasional time sequences that suggest beats. We have studied both the transient and long time behaviour of this simple piston system for a number of different system sizes, piston configurations and initial conditions. A complete list of these numerical results is given in Table I. The observed values of the frequency ω and the damping coefficient λ are obtained by comparing the

Table I. The List of All Simulation Parameters and Results for Each Piston Experiment. The Initial Number Density for Each State Can Be Calculated from the Table Entries and the Equation $n_i = N/(LX_0)$. In the Table the Value ρ_f (see Assumption 2) Is Calculated Using the Enskog Equation. The States Indicated by Bold Face Numbers Are Those for Which $R = M_{gas}/M > 1$

State	N	kT_0	L	X_0	M	g	X_f	kT_f	ρ_f	ω	$\lambda \times 10^3$
1	108	10	20.78	51.96	500	0.4	32.9	46.028	0.209	0.177	1.5
2	108	10	20.78	51.96	1000	0.2	32.9	46.028	0.209	0.128	0.6
3	108	10	29.39	73.48	500	0.4	42.23	67.88	0.100	0.146	1.6
4	108	10	29.39	73.48	1000	0.2	42.22	67.88	0.100	0.1057	0.8
5	108	76.6	29.39	37.5	125	0.4	104.8	45.7	0.037	0.0806	2.0
6	108	76.6	29.39	37.5	500	0.1	104.8	45.7	0.037	0.044	0.5
7(=3)	108	10	29.39	73.48	500	0.4		67.88			1.6
8	108	10	29.39	51.43	1000	0.4	30	89.7	0.151	0.175	
9	108	10	29.39	220.5	100	0.4	126	45.83	0.030	0.072	
9	588	10	68.59	171.5	500	0.4	107	31.9	0.09	0.078	1.3
10	864	1.25	235.15	73.48	4000	0.4	40.28	63.5	0.107	0.157	1.6
11W	432	20	117.58	73.48	125	1.6	62	25.7	0.066	0.164	5.4
12S	432	20	58.78	147	125	0.8	123	25.7	0.066	0.08	1.7
13L	432	20	29.39	293.9	125	0.4	245	25.7	0.066	0.04	0.6
11W	432	20	117.58	73.48	125	0.5	108	14.86	0.036	0.063	2.7
14(=3)	108	10	29.39	73.48	500	0.4	42.6	67.88	0.100	0.146	1.6
15W	432	10	117.57	73.48	2000	0.4	42.6	67.88	0.100	0.155	1.6
16W	864	10	235.15	73.48	4000	0.4	42.6	67.88	0.100	0.148	1.5
17W	1728	10	470.30	73.48	8000	0.4	42.6	67.1	0.1002	0.145	2.0
17W	1728	10	470.30	73.48	1600	2.0	42.6	67.3	0.1002	0.283	7.5
18W	1728	10	470.30	73.48	800	4.0	42.6	67.3	0.1002	0.35	15
19W	1728	10	470.30	73.48	200	16.0	42.6	67.1	0.1002	0.44	30
20W	1728	10	470.30	73.48	100	32.0	42.6	67.3	0.1002	0.465	38
21W	1728	10	470.30	73.48	50	64.0	42.6	67.2	0.1002	0.48	40
22W	1728	5	470.30	73.48	100	16.0	42.6	33.9	0.1002	0.33	27
23W	1728	2.5	470.30	73.48	200	4.0	42.6	16.9	0.1002	0.22	17
24W	432	20	117.58	73.48	4000	0.4	42.6	132.5	0.1002	0.150	1.0
25S	432	20	58.79	147	4000	0.2	85.0	133	0.1002	0.075	0.25
26L	432	20	29.39	293.9	4000	0.1	169	131	0.1002	0.0380	0.06

time evolution of the piston position with a damped cosinusoidal curve, changing parameters until the best fit is obtained.

Scaling Properties

There is an exact scaling property of the microscopic equations of motion of the piston and gas system. That is, for the same initial positions and velocities for the particles and piston, and the same piston geometry and mass, the following transformation leaves the equations of motion invariant

$$\begin{cases} kT \Rightarrow kT/\alpha \Rightarrow (v \Rightarrow v/\sqrt{\alpha}) \\ V \Rightarrow V/\sqrt{\alpha} \\ g \Rightarrow g/\alpha. \end{cases} \tag{88}$$

As the collision rules involve the mass of the particles and the mass of the piston, and these are unchanged, the evolution is identical up to a scaling on the time $t \Rightarrow \sqrt{\alpha}\, t$, which then implies the scaling $\omega \Rightarrow \omega/\sqrt{\alpha}$ and $\lambda \Rightarrow \lambda/\sqrt{\alpha}$. In general, for a different set of initial conditions for the particle's positions and/or velocities, but with the same temperature, we expect the same macroscopic motion of the system (i.e., the same frequency and damping) but with different fluctuations.

This scaling property is verified in our simulations as can be checked by the results listed in Table II. There are two sets of 1728 particle systems (with $X_0 = 73.48$, $X_f = 42.6$, and $L = 470.30$) which satisfy this property. First, the states 20W and 22W differ in initial temperature (and also the final temperature) by a factor of two. This implies that the observed frequency and damping should change by a factor of $\sqrt{2}$. Both of these changes are observed. Second, the states 19W and 23W differ in initial temperature by a factor of four so the frequency and damping should change by a factor of two. Again the frequency and damping do satisfy the

Table II. States that Differ Only by a Scaling of the Temperature

State	N	kT_0	M	g	kT_f	ρ_f	ω	$\lambda \times 10^3$
20W	1728	10	100	32.0	67.3	0.1002	0.465	38
22W	1728	5	100	16.0	33.9	0.1002	0.33	27
19W	1728	10	200	16.0	67.14	0.1002	0.44	30
23W	1728	2.5	200	4.0	16.9	0.1002	0.22	17

predicted scaling relation, and the final temperatures differ by a factor of four.

The Damping Coefficient and Frequency

The observed values of the damping appear to lie within the two extremes; weak damping and strong damping. These two states are typified by 17W and 20W. In a previous paper[12] we have looked at these two states in detail and we find that the important difference is the maximum speed of the piston in comparison to the average thermal velocity of a fluid particle. In the strong damping regime the piston attempts to move faster than the average thermal velocity in its first descent, and carries with it a wave of fluid particles. The momentum carried by this wave of particles travels faster than the piston and is reflected off the bottom of the cylinder, and returned to the piston. The piston then travels back up the cylinder at a speed which is faster than the velocities of many fluid particles, and in this way very few fluid particles can return their increased energy to the piston, thus the piston does not reach its initial position. In one oscillation much of the kinetic energy of the piston has been transferred to the gas and does not return. In contrast, in the weak damping case the motion of the piston is slower than the thermal velocity of the fluid particles and at each stage through the first descent of the piston the fluid is, to a good approximation, able to establish thermal and mechanical equilibrium everywhere within the cylinder. The fluid is compressed until the pressure rises sufficiently to reverse the motion of the piston. As the piston moves more slowly up the cylinder, many fluid particles can collide with it and return much of their energy to the piston. The piston then rises almost to its initial height.

Between these two extremes of weak and strong damping, as characterized above, is a series of intermediate states, and in going from the strong damping state with piston mass 100 to higher piston masses, the initial motion of the piston becomes slower and slower compared with the thermal velocity, and the mechanisms gradually change from those typical of strong damping to those of weak damping.

The principle purpose of this section is to compare the predictions of the kinetic theory developed in previous sections with the results obtained by numerical simulation. In particular, we want to compare in detail the values of the frequency and damping coefficient predicted by Eqs. (43) and (44) with those obtained numerically. We will begin by considering the damping. Let us recall that one of the conclusions obtained from kinetic theory is that introducing the ratio $R = mN/M$, then for $R < \pi$ the damping is weak, while for $R > \pi$ the damping is strong.

As we have investigated two general types of behaviour, strong and weak damping and observed that for 1728 particle systems in particular, the two regimes correspond to $R = N/M > 1$ and $R < 1$, respectively, we can look for relations that fit the behaviour in each regime. The best fit to the numerical data is

$$\begin{cases} \lambda_{\text{fit}} = \dfrac{R}{8}\left(\dfrac{L}{N}\right)^2 \rho_f \sqrt{\dfrac{k_B T_f}{m}} = \dfrac{1}{16}\left(\dfrac{\pi}{2m}\right)^{1/2} \dfrac{L}{N}\, \bar{\lambda}_f & \text{for} \quad R < 1 \quad (89) \\ \lambda_{\text{fit}} = \dfrac{\sqrt{R}}{6}\left(\dfrac{L}{N}\right)^2 \rho_f \sqrt{\dfrac{k_B T_f}{m}} = \dfrac{1}{12}\left(\dfrac{1}{R}\right)^{1/2}\left(\dfrac{\pi}{2m}\right)^{1/2} \dfrac{L}{N}\, \bar{\lambda}_f & \text{for} \quad R > 1 \quad (90) \end{cases}$$

where $\bar{\lambda}_f$ is given by Eq. (43). For $R > 18$, the observed value of λ_{obs} appears to be independent of R. In Fig. 6 we present a graph of all the predicted values of the damping coefficient as a function of the observed value. The two fitted expressions in (89) largely agree with the observed values throughout their expected ranges of validity, although there are some points in $R < 1$ region where the fit valid for $R > 1$ agrees well with the observed values. Let us note that both expressions (89) and (90) give the same result for $R = 16/9 \cong 1.8$.

In Fig. 6 we present a graph of the damping coefficient computed from the different expressions (43), (89), and (90) as functions of the observed value λ_{obs}. As can be seen on this figure the expressions (89) and (90) largely agree with the observed values throughout their ranges of validity, i.e., $\lambda_{\text{fit}} \cong \lambda_{\text{obs}}$. On the other hand the values predicted from (43) are about 115 too large, i.e., $\bar{\lambda}_f \cong 115\lambda_{\text{obs}}$. (We shall come back to this point after Fig. 9.)

In Fig. 7 we present a comparison between the predicted results for the frequency and the observed values (Table I). If the friction coefficient is sufficiently small, then the predicted frequency of oscillations obtained from (43) is approximately

$$\omega_{\text{ad}} = \sqrt{2R}\,\frac{L}{N}\,\rho_f \sqrt{k_B T_f} \tag{91}$$

(since in all our simulations the coefficient $\frac{1}{2}(c/X_f)^2$ is negligible). Let us note that the frequency given by Eq. (91) is exactly the frequency obtained in thermodynamics assuming adiabatic oscillations.[11]

As we can see from Fig. 7, the adiabatic frequency (91) agrees very well with the observed values for $R < 1$. This corresponds to the case of weak damping with λ_{obs} in the range $(0.6\text{–}2) \times 10^{-3}$. Let us remark that another measure of weak versus strong damping is given by the ratio

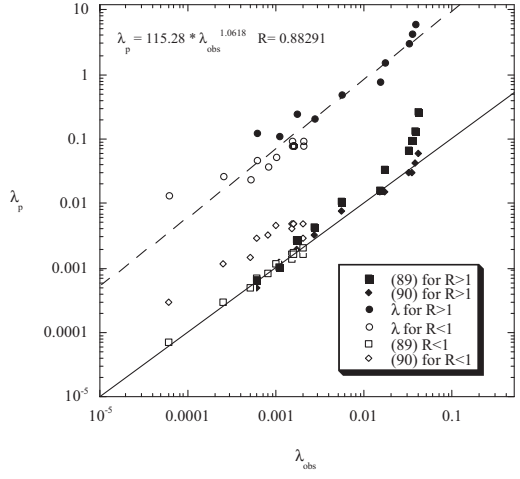

Fig. 6. A log–log plot of the values predicted by Eqs. (43), (89), and (90) as functions of the numerically observed value λ_{obs}. The empty symbols are for those states with $R < 1$, the filled symbols are for those with $R > 1$. Notice that the empty squares and the full diamonds lie along the diagonal, which is the line of agreement between the predicted values (89) and (90) and the observed values. The equation in the top left-hand side is a power law fit to the data which indicates that to a good approximation $\lambda_p \sim 115\lambda_{\text{obs}}$.

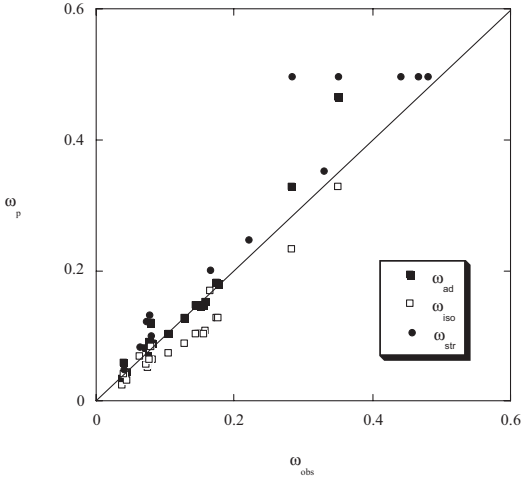

Fig. 7. A graph of ω_{ad}, and of ω predicted by Eqs. (91), (92), and (93), as functions of the observed frequency ω_{obs}.

$\lambda_{\text{obs}}/\omega_{\text{obs}}$, and for the simulations with $R<1$ this ratio lies in the range $(1\text{–}15)\times 10^{-3}$.

However, for $2<R<5$, the observed values are best fitted by

$$\omega_{\text{iso}} = \sqrt{R}\,\frac{L}{N}\,\rho_f\,\sqrt{k_B T_f} \qquad \text{for} \quad 2<R<5 \tag{92}$$

which corresponds to the thermodynamical value, assuming isothermal oscillations. For this range of R, the damping is intermediate between weak and strong with $\lambda_{\text{obs}}/\omega_{\text{obs}}$ in the range $(20\text{–}40)\times 10^{-3}$.

Finally for $R>5$, the observed values are best fitted by the expression independent of R

$$\omega_{\text{str}} = \frac{\pi}{\sqrt{2}}\,\frac{L}{N}\,\rho_f\,\sqrt{k_B T_f} \qquad \text{for} \quad R>5. \tag{93}$$

It corresponds to strong damping with λ_{obs} larger than 17×10^{-3} and a ratio $\lambda_{\text{obs}}/\omega_{\text{obs}}$ larger than 70×10^{-3}.

There is one sequence of simulations with 1728 particles at initial temperature $k_B T_0 = 10$ in a cylinder of width 470.3 and initial piston position of $X_0 = 73.48$ where we can follow the progression from weak damping in state 17W to strong damping in state 21W. For all of these simulations we have the same final equilibrium state: $X_f = 42.6$, $kT_f = 67.2 \pm 0.1$, and $\rho_f = 0.1002$. From Eq. (43) it can be shown that $\bar{\lambda}_f \approx 615 M^{-1}$, and from (91) $\omega_{\text{ad}} = 13.14/\sqrt{M}$. Using the values from Eqs. (89) and (90) for λ_{fit}, and from Eqs. (91)–(93) for ω_{fit} we obtain the results presented in Table III.

Only for the weak damping state (17W) does the predicted frequency ω_{ad} agree with the observed frequency; for the intermediate damping state (18W) the isothermal frequency agrees with the observed value, while for

Table III. Results for the Sequence of States with the Same Final State and Same Value of *Mg*. The Value of λ_{fit} Is the One that Is Valid for the Value of *R*

State	M	R	g	ω_{obs}	ω_{ad}	ω_{fit}	$\lambda_{\text{obs}}\times 10^3$	$\bar{\lambda}_f \times 10^3$	$\lambda_{\text{fit}}\times 10^3$
17W	8000	0.216	0.4	0.145	0.147	0.147	2.0	77	1.6
17W	1600	1.08	2.0	0.283	0.327	0.232	7.5	386	10.6
18W	800	2.16	4.0	0.35	0.465	0.329	15	769	15.2
19W	200	8.64	16.0	0.44	0.929	0.50	30	3080	30.4
20W	100	17.28	32.0	0.465	1.314	0.50	38	6150	42
21W	50	34.56	64.0	0.48	1.858	0.50	40	12300	43

strong damping the observed frequency remains constant. For the damping coefficients the value of $\bar{\lambda}_f$ never agrees with the observed value.

In attempting to fit the motion of the piston to a damped cosine for many of the strong damping states it was found that a much better fit could be obtained if the initial displacement of the piston was not included in the fit, that is, if the initial displacement for the purposes of the fit was taken to be less than the actual displacement. In Fig. 8 we show a comparison of the actual piston motion and the damped cosinusoidal fit to that motion for the first two oscillations of the piston. Notice that the actual piston motion is not cosinusoidal but has narrower troughs and broader peaks, and this is most noticeable in the weak damping case. In general the fits are quite reasonable except for the weak damping case in which a fit to the first two oscillations is different to the fit to the whole transient region. This occurs either because the damping is not constant over the whole transient, or there are significant fluctuations. However, for this case the piston has mass 8000 and fluid has mass 1728 so the largest fluctuations should be in the component with the smallest mass, i.e., the fluid.

Velocity of the Piston

From the sequence of plots of the piston velocity in Fig. 9 it is evident that for the strong damping states where $R = 34.56$, 17.28, and 8.64 (i.e., $M = 50$, 100, and 200) after the piston is released the velocity increases (in absolute value) almost immediately to a maximum value $V_{\max} = 8.5$ and remains at that velocity for 6 time units. Since in this time interval no recollisions of the particles with the piston has yet taken place, we can compare this $V_{\max}$ with the terminal velocity V_∞ for the piston in an infinite cylinder. Using Eq. (23) we find $V_\infty = 7.3$ which is in rather good agreement with the (constant) velocity of the piston in its first descent. Other values for strong damping are presented in Table IV.

This comparison indicates that the friction mechanism leading to a constant velocity for the infinite cylinder, or during the first descent, is different from the mechanism leading to the observed damped oscillations. In fact, as the piston descends the cylinder we have seen[12] that in the strong damping case 22W a region of higher density builds up in front of the piston. Using fluid hydrodynamics[14] we find that in 2-dimensions a constant velocity leads approximately to a density in front of the piston two times higher than the initial density.

This is in fact the mechanism which leads to the friction coefficient $\bar{\lambda}_f$. However, in ref. 12 we observe that the maximum density at the surface of the piston is typically three times higher than the initial density. (Rather than using Eq. (24) to calculate the terminal velocity, if take the terminal

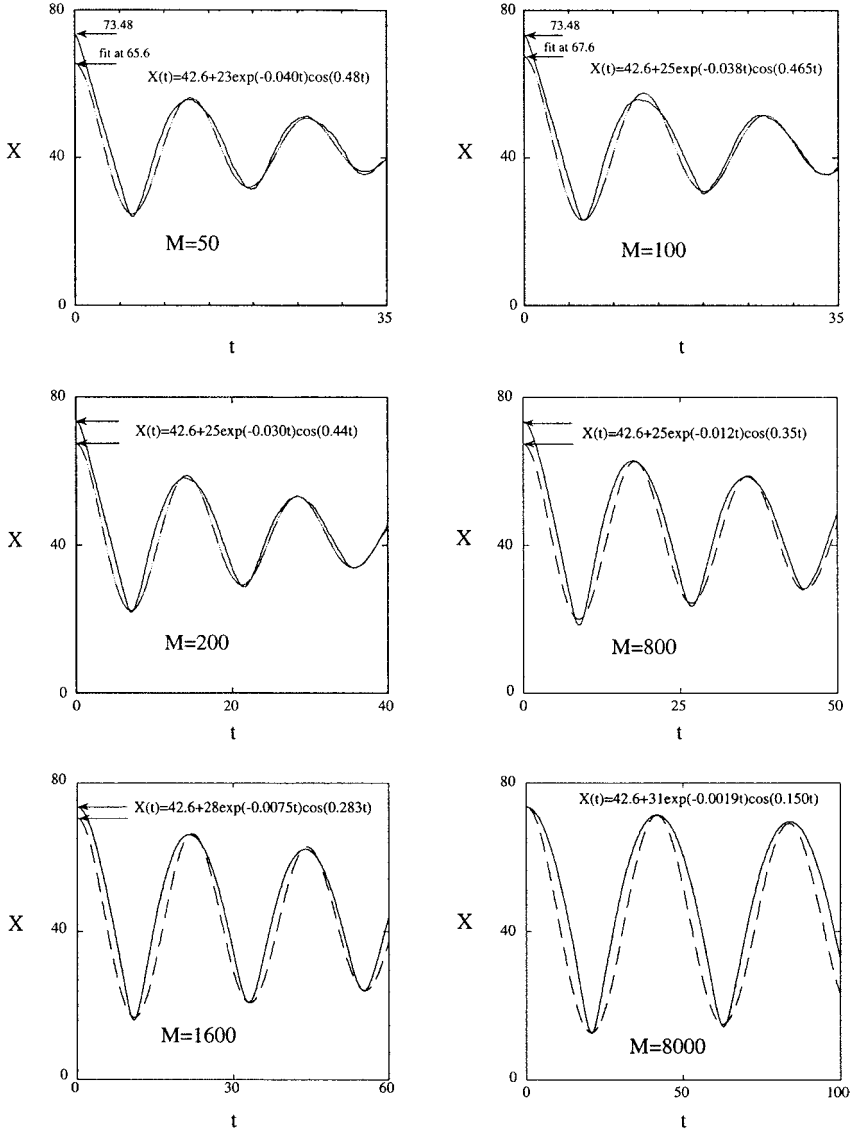

Fig. 8. The time evolution of the piston for the sequence of 1728 particle states. The $M = 8000$ is the weak damping state and the $M = 100$ is the typical strong damping state. The solid line is the position of the piston and the dashed line is the damped cosinusoidal fit to the piston position. The arrows on the vertical axes in the first five states indicate that the best fit to the whole piston motion is obtained by changing the initial piston position. Both the real piston position and the changed value are indicated by arrows on the x-axis.

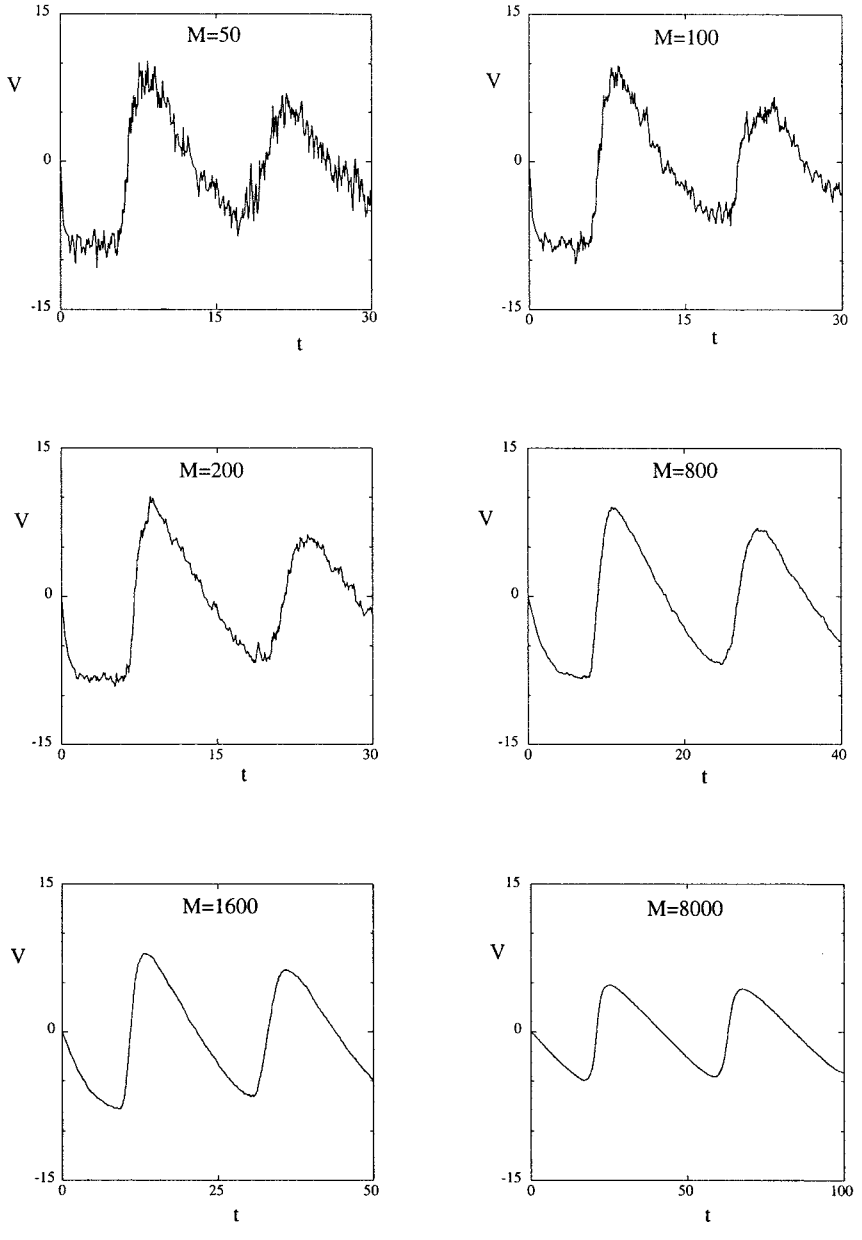

Fig. 9. The velocity of the piston for the sequence of 1728 particle states. The $M = 8000$ is the weak damping state and the $M = 100$ is the typical strong damping state. Notice that in the first three states the piston has reached its maximum velocity in the first compression.

Table IV. Comparison of the Velocity of the Piston in the Infinite Cylinder (Eq. (29)) and the Observed Value During the First Descent

State	R	V_∞	$V_{\max}$
18W	2.16	7.3	7.6
19W	8.64	7.3	8.5
20W	17.28	7.3	8.3
21W	34.56	7.3	8.8
22W	17.28	5.2	5.8
23W	8.64	3.7	4.2

velocity to be -8.5 and use this to determine the density increase we get $\rho_0 = 0.129$. This is well within a three fold density increase.)

It is apparent that when the piston reaches its terminal velocity it is no longer acting as a damped oscillator but rather the force acting on it is dissipated by the fluid. Once this initial damping is complete and the piston remains below V_∞, its behaviour is much more like a damped oscillator. We could assume that the damped oscillation begins when this phase is complete, or as we have done, assume that the piston begins at a smaller value of X. We have already seen that this is necessary to get realistic fits to the piston motion.

7. CONCLUSIONS

In this paper we have investigated some fundamental questions concerning the approach to equilibrium and the entropy production for systems which initially are away from equilibrium. For the simple piston considered in this work we have in particular obtained from the Boltzmann equation, as well as from numerical simulations, an approach towards the equilibrium position of the piston predicted by thermostatics.

As observed in recent experiments,[8] our analytical equations and all our simulations clearly indicate that two regimes are exhibited: a weak damping regime and a strong damping regime, depending on the ratio R of the mass of the gas to the mass of the piston (small or large). For weak damping, the frequency of oscillations observed in the simulations are in good agreement with the values calculated from the Boltzmann equation, and correspond to both the value obtained from hydrodynamics using the adiabatic hypothesis and those observed experimentally. On the other hand, for intermediate damping our simulations seem to indicate isothermal oscillations as observed in recent experiments. Finally, for strong

damping the observed oscillations do not depend any more on the ratio R. To understand the microscopic origin of the difference between weak and strong damping, we have plotted the velocity of the piston as a function of time. It shows that for weak damping the velocity of the piston varies slowly with the consequence that the energy which has been transferred to the gas can be transferred back to the piston. While in the case of strong damping the velocity of the piston varies very rapidly and leads to dissipation. The observed velocity of the piston before recollision of the molecules (on the piston) agrees well with the predicted value and thus the friction coefficient computed from the microscopic theory agrees with the simulations. However, the predicted values of the damping coefficient appear too large by two orders of magnitude regardless of the initial state. Independently of weak or strong damping the simulations have shown that the evolution takes place in two distinct stages: in the first stage the evolution appears to be a deterministic transient motion with damped oscillations toward the equilibrium position where the pressure of the gas balances the external force. In the second stage we observe steady fluctuations around the equilibrium position with a single frequency equal to the frequency in the transient stage, but the amplitude of which is modulated at random and slowly decreases in time with occasional sequences suggesting beats. We interpret these random fluctuations as the mechanism which will ultimately lead to a Maxwellian velocity distribution of the gas particles.

In our microscopical model we have introduced *ad hoc* assumptions to obtain explicit equations for the evolution. We have shown that one can analyse the equations so obtained by means of an entropy function which has all the properties required from thermodynamics in particular there is a positive entropy production during the evolution, the entropy is a maximum at equilibrium and Onsager's relations are satisfied near equilibrium. To go further it appears necessary to investigate in detail the coupled equations for the piston and the fluid; the entropy should then be defined by taking into account the fact that the fluid is inhomogeneous. One can expect that the definitions and assumptions we have used should be good when the system is close enough to equilibrium, or when the parameters are chosen such that the velocity of the piston is sufficiently small to insure that at any time the fluid is approximately homogenous. However even in this case it is still an open problem.

ACKNOWLEDGMENTS

Ch. Gruber greatly acknowledges the kind hospitality at the University of New South Wales where this work began and G. P. Morriss greatly acknowledges the hospitality at the Institute of Theoretical Physics of the

École Polytechnique Fédérale de Lausanne where part of this research was performed.

REFERENCES

1. E. H. Lieb and J. Yngvason, The physics and mathematics of the second law of thermodynamics, *Phys. Rep.* **310**:1 (1999).
2. Ch. Gruber, Thermodynamics of systems with internal constraints, *European J. Phys.* **20**:259 (1999).
3. E. H. Lieb, Some problems in statistical mechanics that I would like to see solved, *J. Stat. Phys.* **263**:491 (1999).
4. Ch. Gruber and L. Frachebourg, On the adiabatic properties of a stochastic adiabatic wall: Evolution, stationary non-equilibrium, and equilibrium states, *Physica A* **272**:392 (1999).
5. Ch. Gruber, S. Pache, and A. Lesne, Deterministic motion of the controversial piston in the thermodynamic limit, *J. Stat. Phys.* **108**:669 (2002).
6. Ch. Gruber, S. Pache, and A. Lesne, Two-time-scale relaxation towards thermal equilibrium of the enigmatic piston, preprint (2002).
7. E. Rüchardt, *Phys. Z.* **30**:58 (1929).
8. O. L. de Lange and J. Pierrus, *Amer. J. Phys.* **68**:265 (2000).
9. G. P. Morriss and Ch. Gruber, Strong and weak damping in the adiabatic motion of the simple piston, *J. Stat. Phys.* **109**:549 (2002).
10. J. Piasecki and Ch. Gruber, From adiabatic piston to macroscopic motion induced by fluctuations, *Physica A* **265**:463 (1999).
11. L. D. Landau and E. M. Lifshitz, *Fluid Mechanics* (Pergamon Press, 1959).
12. J. A. Barker and D. Henderson, What is "liquid"? Understanding the states of matter, *Rev. Modern Phys.* **48**:587 (1976).